Dental Materials xxx (xxxx) xxx

Contents lists available at ScienceDirect

Dental Materials

journal homepage: www.elsevier.com/locate/dental

Evaluation of flexible three-dimensionally printed occlusal splint materials: An in vitro study

Leila Perea-Lowery [a,*], Mona Gibreel [a], Sufyan Garoushi [a], Pekka Vallittu [a,b], Lippo Lassila [a]

[a] Department of Biomaterials Science and Turku Clinical Biomaterials Centre-TCBC, Institute of Dentistry, University of Turku, Turku 20520, Finland
[b] City of Turku Welfare Division, Oral Health Care, Puolalankatu 5, 20101 Welfare Division, Turku FI-20101, Finland

ARTICLE INFO

Keywords:
Three-dimensional printing
Splints
Flexural strength
Wear
Water sorption

ABSTRACT

Objective: To evaluate and compare the mechanical properties, water sorption, water solubility, and degree of double bond conversion of three different commercially available three-dimensional (3D) printing resins used for the fabrication of flexible occlusal splints.
Methods: A digital printer was used to generate specimens from the evaluated splint materials (KeySplint Soft, IMPRIMO LC Splint flex, and V-Print splint comfort). The specimens were equally divided and tested either dry or after water storage at 37 °C for 30 days. A three-point bending test was used to assess flexural strength, elastic modulus, and fracture toughness. A two-body wear test was performed using a dual-axis chewing simulator. Water sorption and water solubility were measured after 30 days. The degree of double bond conversion was determined by FTIR-spectrometry. All data for the evaluated properties were collected and statistically analyzed.
Results: Both material and storage conditions had a significant effect on the flexural strength ($P < 0.001$), elastic modulus ($P < 0.001$), fracture toughness ($P < 0.001$), and wear ($P < 0.001$). The highest water sorption was noticed with IMPRIMO LC Splint flex (1.9 ± 0.0 %), while V-Print splint comfort displayed the lowest water solubility (0.2 ± 0.0 %). For the degree of conversion, it was statistically non-significant among the different materials ($P = 0.087$).
Significance: Different flexible 3D-printed splints available in the market displayed variations in the evaluated properties and clinicians should consider these differences when choosing occlusal device materials. Among the tested flexible splint materials, KeySplint Soft had the greatest flexural strength, elastic modulus, fracture toughness, wear resistance, and degree of conversion. It also showed the lowest water sorption.

1. Introduction

Splint therapy can be defined as the art and science of using removable appliances to achieve neuromuscular harmony in the masticatory system and to create a mechanical disadvantage for parafunctional forces [1]. Splints have been recommended for therapeutic treatments of temporomandibular disorders (TMDs), craniomandibular disorders (CMDs), and to reduce tooth wear in patients experiencing bruxism [2–5]. Intra-oral occlusal splints are intended to provide a uniform and balanced occlusal contact without permanently changing the mandibular rest position or the dental occlusion. In addition, a well-designed splint promotes a harmonic relationship between the masticatory muscles, disk assemblies, joints, ligaments, bone, teeth, and tendons [1,6].

Occlusal splints are designed to cover the occlusal and incisal surfaces of the teeth in the upper and/or lower jaw [7]. The use of vacuum-formed ethylene vinyl acetate (EVA) soft splints has been associated with a high degree of patient tolerance [8]. Their use is justified by the rationale that the soft, resilient material demonstrates a shock-absorbing capacity, which may dissipate heavy loads associated with parafunctional habits [7,9,10].

Additive manufacturing (AM) is the process of fabricating 3D objects in a layer-by-layer fashion directly by employing computer-aided design (CAD) data. Such technology has gained widespread acceptance in a broad range of biomedical fields [11–14]. The diverse techniques, as well as the wide range of employed materials with varying physical characteristics, make AM approaches very appealing for a variety of applications [15]. In addition, the design freedom associated with it allows for the production of complex structures that would be difficult to construct using standard subtractive manufacturing methods [16,17].

* Correspondence to: Itäinen Pitkäkatu 4B (2nd floor), Turku FI-20520, Finland.
E-mail address: leila.perea@utu.fi (L. Perea-Lowery).

https://doi.org/10.1016/j.dental.2023.08.178
Received 2 November 2022; Accepted 23 August 2023

Table 1
Materials evaluated identified by the manufacturer, indications, printer compatibility, and chemical composition as provided by manufacturer.

Material	Manufacturer	Indication as mentioned by manufacturer	Printer compatibility	Chemical composition from the manufacturer safety data sheet	Mass %
KeySplint Soft	Keystone GmbH, Singen, Germany	Bite planes Mouthguards Nightguards Snoring appliances Splints Repositioners	DLP printers with 385 and 405 nm light sources.	***Methacrylate-based resin*** Proprietary ingredient #1 Proprietary ingredient #2 Proprietary ingredient #3	 ≥25–≤50 ≤3 ≤3
IMPRIMO LC Splint flex	Scheu-Dental GmbH, Iserlohn, Germany	Occlusal splints Bruxism and lower jaw protrusion splints	DLP printers with 385 nm light source.	***Methacrylate-based resin*** Methacrylate monomer 1 Methacrylate monomer 2 Methacrylate monomer 3 Photoinitiator	 <60 <40 <2 2
V-Print splint comfort	VOCO GmbH, Cuxhaven, Germany	Therapeutic splints Auxiliary and functional parts for diagnostics Bleaching splints (home bleaching) Palatal plates	DLP printers with 385 nm light source.	***Acrylate-based resin*** Aliphatic acrylate Triethylene glycol dimethacrylate Diphenyl-(2,4,6-trimethylbenzoyl) phosphine oxide	 25–50 5–10 ≤2.5

Therefore, 3D printing has been commonly used in the fabrication of digital occlusal splints [3,18,19].

A wide range of 3D printing-compatible materials (flexible, conductive, magnetic, ferromagnetic, and with shape memory) has recently emerged [15,20]. For example, EVA, which has been successfully employed in 3D printing [21]. Furthermore, photocurable elastomers are now commercially accessible for different applications [22–24]. These elastomers are based on ultraviolet (UV) curable urethane acrylates and acrylates with flexible chains that give the flexible domains in the cured elastomer network [24]. By adjusting the combination of urethane and acrylate monomers, the elongation of 3D-printed elastomers can be vastly enhanced [25]. Accordingly, new materials intended for the production of digital flexible occlusal splints have been released to the market.

The aim of this in vitro study was to evaluate and compare the mechanical properties, water sorption, water solubility, and degree of double bond conversion of three different commercially available 3D printing resins used for the fabrication of flexible occlusal splints. The null hypothesis was that all the tested flexible 3D printed splint materials would display similar properties.

2. Materials and methods

2.1. Specimens preparations

In this study, the flexural strength, elastic modulus, fracture toughness, wear, water sorption, water solubility, and degree of double bond conversion were assessed for three different flexible splint materials used for 3D printing (Table 1). A digital light processing (DLP) printer (Asiga MAX™, SCHEU-DENTAL GmbH, Iserlohn, Germany) was used to generate specimens from the evaluated materials: KeySplint Soft, IMPRIMO LC Splint flex, and V-Print splint comfort. The printing was performed at 90° to the building platform with a layer thickness of 100 μm. All specimens were cleaned in an ultrasonic bath (Quantrex® 90, L&R Ultrasonics, Kearny, NJ, USA) filled with 97 % isopropanol for 10 min, and then dried with compressed air before post-curing with a light emitting diode (LED) device at 60 °C for 30 min (Form cure, formlabs, Berlin, Germany). The specimens were then ground to the final dimensions using successive silicon carbide paper grits up to P1200 (Struers, Copenhagen, Denmark). Specimens were equally divided and tested either dry or after water-storage at 37 °C for 30 days.

2.2. Ultimate flexural strength and elastic modulus

The ultimate flexural strength and elastic modulus were measured by conducting a three-point bending test in accordance with international standards organization (ISO) 20795-1 [26] using a universal testing machine (Model LRX, Lloyds Instruments Ltd., Hampshire, UK). The specimens' final dimensions were 65.0 mm × 10.0 mm × 3.3 mm (n = 16/material). The specimens were fixed between two test supports separated by 50.0 mm and loaded at a crosshead speed of 5.0 mm/min. The load-deflection curves were recorded using computer software (Nexygen 4.0, Lloyd Instruments Ltd., Hampshire, UK). Each test was detected to be finished when the load was reduced to 10 % of the maximum load or when the deflection of the specimen reached 15.0 mm. Ultimate flexural strength (σ) and elastic modulus (E) values were obtained in MPa according to the following formulas [27]:

$$\sigma = \frac{3FI}{2bh^2} E = \frac{F_1 I^3}{4bh^3 d} \quad (1)$$

where $\boldsymbol{F}$ is the maximum load (newtons) applied to the specimen, $\boldsymbol{I}$ is the span length (millimeters), $\boldsymbol{b}$ is the width of the test specimen (millimeters), $\boldsymbol{h}$ is the thickness of the test specimen (millimeters), $\boldsymbol{F_1}$ is the load (newtons) at a point in the straight line portion of the load/deflection curve, and $\boldsymbol{d}$ is the recorded deflection (millimeters) at load $\boldsymbol{F_1}$.

2.3. Fracture toughness (KIC)

Fracture toughness (K_{IC}) measurement was performed on single-edge notched bend (SENB) specimens with dimensions of 4.0 × 8.0 × 40.0 mm^3 and a pre-crack of 3.0 ± 0.2 mm (n = 14/material). The specimens were exposed to a three-point bending test using a universal testing machine (Model LRX, Lloyds Instruments Ltd., Hampshire, UK). The test settings were adjusted to make a displacement rate of 1.0 mm/min, while the test span was set to 32.0 mm. The maximum stress intensity factor was calculated (MPa $m^{1/2}$) using the maximum recorded force according to the following formulas [28]:

$$k_{IC} = \frac{f P_{\max} l_t}{b_t h_t^{3/2}} \times \sqrt{10^{-3}} \quad (2)$$

where P_{max} is the maximum load exerted on the specimen (newtons), l_t is the span length (millimeters), b_t is the specimen width (millimeters), h_t is the specimen height (millimeters), and $\boldsymbol{f}$ is a geometrical function dependent on $\mathbf{x}$: $f(x) = 3x^{1/2}\ [1.99 - x(1-x)(2.15 - 3.93x + 2.7x^2)]/[2(1 + 2x)(1 - x)^{3/2}]$, $x = a/h_t$, and $\mathbf{a}$ is the pre-crack length (millimeters).

Representative fractured specimens from each material were sputtered with a gold coating using a sputter coater (BAL-TEC SCD 050 Sputter Coater, Balzers, Liechtenstein) and then characterized using a scanning electron microscope (SEM) operated with an accelerating

Table 2
Properties of evaluated flexible 3D splint materials.

Material	Flexural strength (MPa)		Elastic modulus (GPa)		Fracture toughness (MPa $m^{1/2}$)		Degree of double bond conversion %
	Dry	*Water*	*Dry*	*Water*	*Dry*	*Water*	
KeySplint Soft	29.9 ± 1.6^{aA}	24.4 ± 3.3^{aB}	0.8 ± 0.1^{aA}	0.5 ± 0.1^{aB}	2.3 ± 0.5^{aA}	1.1 ± 0.3^{aB}	81.8 ± 5.1^{a}
IMPRIMO LC Splint flex	26.3 ± 1.6^{bA}	4.7 ± 1.4^{bB}	0.8 ± 0.1^{aA}	0.2 ± 0.1^{bB}	1.1 ± 0.1^{bA}	0.4 ± 0.1^{bB}	72.5 ± 9.5^{a}
V-Print splint comfort	26.0 ± 2.0^{bA}	10.4 ± 2.0^{cB}	0.8 ± 0.1^{aA}	0.2 ± 0.1^{bB}	1.1 ± 0.1^{bA}	0.5 ± 0.0^{bB}	69.4 ± 9.5^{a}
*P value (One-way ANOVA)	<0.001	<0.001	0.913	<0.001	<0.001	<0.001	0.087

Same superscript lowercase letters indicate statistically similar materials in the same column ($P > 0.05$).
Same superscript uppercase letters indicate statistical similarity between dry and water-stored specimens in the same raw ($P > 0.05$).
* $P < 0.05$ significant.

voltage of 15.0 KV (SEM, JSM 5500, Jeol Ltd., Tokyo, Japan).

2.4. Two-body wear

A two-body wear test was performed on specimens prepared with dimensions of 2.0 × 10.0 × 15.0 mm^3 (n = 4/material). Each specimen was fixed to an acrylic resin block and sequentially polished using silicon carbide sheets with grain sizes up to 4000 grit FEPA. The specimens were stored in water at 37 °C for 24 h before testing. A chewing simulator (CS-4.2, SD Mechatronik, Feldkirchen-Westerham, Germany) with two chambers was used to conduct the wear test in the presence of water. The specimens were fixed to the lower plastic holder of the simulator while the manufacturer's standard loading tips (Steatite ball, 6.0 mm) were secured to the upper one with a fastening screw. A chewing simulation was performed at 1.5 Hz with a vertical weight of 2 kg, which is equivalent to 20.0 N of chewing force. Each specimen was subjected to 15,000 loading cycles. The wear patterns were then scanned with a 3D optical microscope (Bruker Nano GmbH, Berlin, Germany) and the material loss estimates were calculated using Vision64 Map software. The total vertical wear depth values were acquired in micrometers (μm) from several sites by averaging the deepest points of all profile scans.

2.5. Water sorption and water solubility

To assess water sorption and water solubility, the specimens (n = 8/material) were dried in a vacuum desiccator containing freshly dried silica at 37 ± 1 °C for 22 h and subsequently at 23 ± 1 °C for two hours. The measurements were taken from the same specimens used for flexural strength measurements. To determine the initial weight (m_1), the specimens were weighed on a digital analytical balance (XS105, Mettler Toledo, Greifensee, Switzerland). The drying process was repeated until the difference between consecutive weight measurements was less than 0.1 mg. Subsequently, the specimens were immersed in 50 mL of distilled water and kept at 37 °C for 30 days. Weighting of the specimens was performed at 1, 2, 3, 7, 14, 21, 28, and 30 days (m_2) after being taken out of the water and meticulously dried with absorbent paper for 60 s. Finally, the specimens were re-dried until they reached a final consistent mass (m_3). The water sorption and solubility percentages were calculated from the following equations [29]:

$$Sorption(\%) = 100 \times \frac{m_2 - m_3}{m_1} \quad Solubility(\%) = 100 \times \frac{m_1 - m_3}{m_1}, \tag{3}$$

where $\mathbf{m_1}$ is the dry mass (gram) of the specimen after storing it in a desiccator for 24 h, $\mathbf{m_2}$ is the mass (gram) of the specimen after water immersion for 30 days, and $\mathbf{m_3}$ is the constant mass (gram) of the specimen after the second drying cycle.

2.6. Degree of double bond conversion (C═C)

The degree of double bond conversion (DC) was measured using a Fourier transform infrared spectrometer (Frontier FT-IR spectrometer, PerkinElmer, Llantrisant, UK) (n = 5/material). The measurements were performed on the uncured material and on the top surface of each specimen. The absorbance intensity ratio of the methacrylate (C═C) peak at 1638 cm^{-1} and the carbonyl bond (C═O) peak at 1720 cm^{-1} was used as the internal standard for polymerized and unpolymerized splint materials. The absorbance was measured in 16 scans at a resolution of 4.0 cm^{-1} from 650 to 4000 cm^{-1}. The DC was calculated as follows [30]:

$$DC(\%) = 100 \times \left(1 - \frac{(C_{1638}|C_{1720})polymerized}{(C_{1638}|C_{1720})unpolymerized}\right) \tag{4}$$

2.7. Statistical analysis

All data for the evaluated properties were collected and normality distribution was tested. The data were statistically analyzed with a statistical software program (IBM SPSS Statistics, v24; IBM Corp., Armonk, NY) using ANOVA followed by Tukey's HSD post hoc test for pair-wise comparison (α = 0.5). Independent samples t test was used to compare the values of dry and water-stored specimens for each material. A Pearson correlation coefficient was calculated to estimate the relationship between wear and the investigated mechanical properties, including flexural strength and fracture toughness.

3. Results

Both the material and the storage conditions had a significant impact on the flexural strength ($P < 0.001$), elastic modulus ($P < 0.001$), and fracture toughness ($P < 0.001$). Mean values and standard deviations of flexural strength, elastic modulus, fracture toughness, and degree of double bond conversion are presented in Table 2.

Among the flexible splint materials investigated, KeySplint Soft displayed significantly the highest dry flexural strength when compared to IMPRIMO LC Splint flex ($P = 0.001$) and V-Print splint comfort ($P = 0.001$). The three splint materials had the same mean value of dry elastic modulus (0.8 GPa, $P = 0.913$). All the investigated materials displayed a substantial drop in flexural strength and elastic modulus ($P < 0.05$) after water storage. The flexural strength of KeySplint Soft decreased from 29.9 to 24.4 MPa (19 %), whereas it decreased from 26.3 to 4.7 MPa (82 %) for IMPRIMO LC Splint flex and from 26.0 to 10.4 MPa (60 %) for V-Print splint comfort. However, none of the specimens fractured during the three-point bending test, but they showed elastic rebound after a few minutes from load removal. Furthermore, the elastic modulus of the water-stored KeySplint Soft specimens was statistically higher than IMPRIMO LC Splint flex ($P < 0.001$) and V-Print splint comfort ($P < 0.001$), while IMPRIMO LC Splint flex and V-Print splint comfort were statistically similar ($P = 0.374$).

Regarding fracture toughness (K_{IC}), the dry specimens of KeySplint Soft had the highest significant value of 2.3 MPa $m^{1/2}$ ($P < 0.001$), while the other two materials displayed a similar critical intensity factor of 1.1 MPa $m^{1/2}$ ($P = 0.926$) (Table 2). A critical decrease in fracture toughness was noticed after water storage for all the materials, and the IMPRIMO LC Splint flex splint material had the lowest fracture

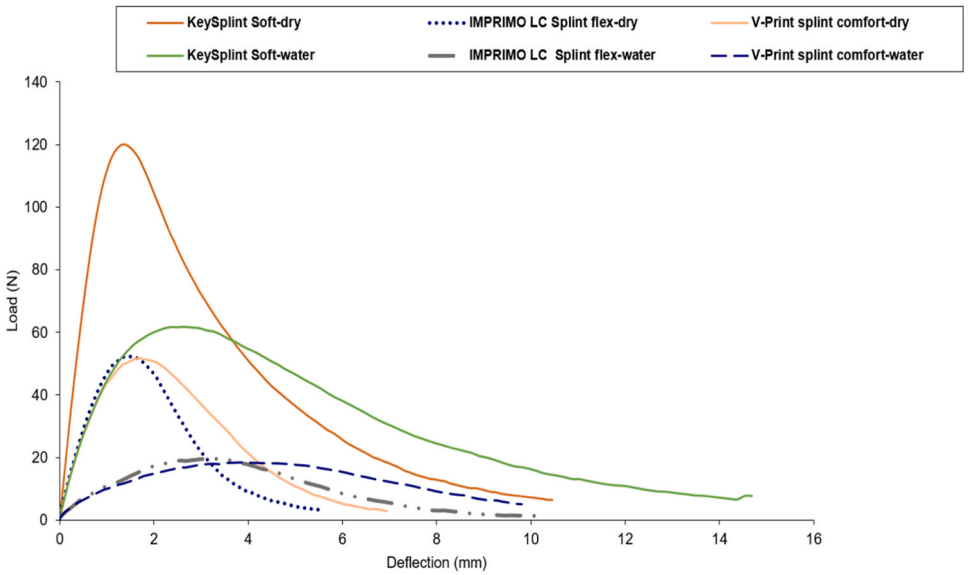

Fig. 1. Load/deflection curves obtained during fracture toughness test of evaluated flexible 3D-printed splint materials.

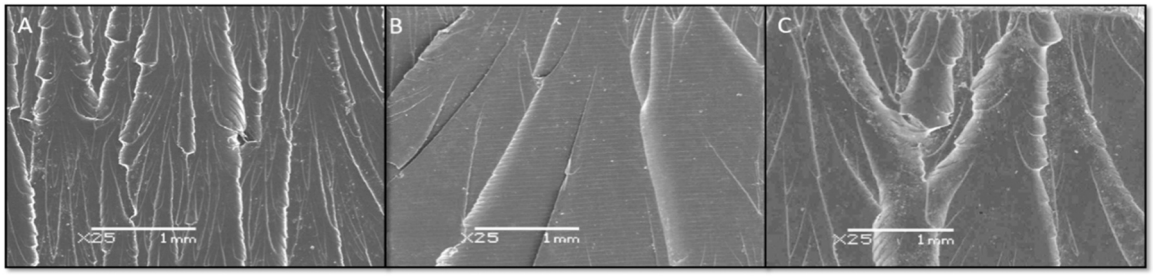

Fig. 2. SEM micrographs (x25, 15.0 KV) of fracture surfaces after fracture toughness test. A, IMPRIMO LC Splint flex; B, KeySplint Soft; C, V-Print splint comfort.

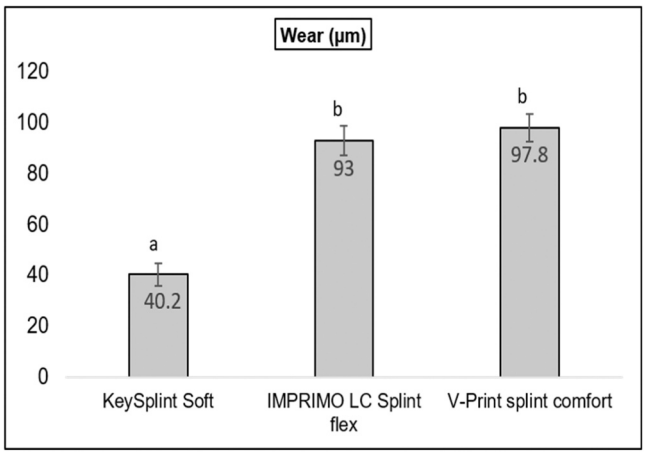

Fig. 3. Mean values of vertical wear depth (µm) of evaluated 3D-printed flexible splint materials. Same letters indicate statistically similar materials ($P > 0.05$).Error bars represent standard deviations.

toughness, being statistically relevant only with KeySplint Soft ($P < 0.001$). The load-displacement curves obtained from the fracture toughness testing of the investigated materials are presented in Fig. 1. They tended to show a quite linear elastic behavior that ended with a maximum load. Beyond that, the specimens showed a progressive decrease in load carrying capacity until the test ended. None of the specimens displayed complete fracture after fracture toughness testing. When compared to the other two materials, KeySplint Soft exhibited the highest peak load and displacement. Furthermore, regardless of the material type, the plasticizing action of water on the water-stored specimens resulted in a greater displacement. Fig. 2 presents the SEM micrographs of the fractured specimens of the three evaluated materials, which showed that the propagated cracks formed some patterns and layers instead of a flat surface, indicating that the materials displayed resistance against the applied load.

Vertical wear depth values were statistically significant ($P < 0.001$) among different materials (Fig. 3). KeySplint Soft displayed the lowest significant vertical wear depth (40.2 ± 4.4 µm) which was even less than half of the values displayed by IMPRIMO LC Splint flex (93 ± 5.8, $P < 0.001$) and V-Print splint comfort (97.8 ± 5.4, $P < 0.001$). IMPRIMO LC Splint flex and V-Print splint comfort had statistically similar vertical wear depth values ($P = 0.565$). In addition, wear facets varied in size, with that of KeySplint Soft being the smallest as seen in Fig. 4. Wear was strongly and negatively correlated with flexural strength ($r^2 = -0.703$, $P = 0.01$) and fracture toughness ($r^2 = -0.969$, $P < 0.001$).

Fig. 5 shows the results of water sorption and solubility percentages. The lowest water sorption was found for KeySplint Soft (1.1 ± 0.2 %), while the highest water sorption was noticed with IMPRIMO LC Splint flex (1.9 ± 0.0 %), being significantly higher than KeySplint Soft ($P < 0.001$) and V-Print splint comfort ($P < 0.001$). V-Print splint comfort displayed the lowest water solubility (0.2 ± 0.0 %), while KeySplint Soft and IMPRIMO LC Splint flex were statistically non-significant (0.5 ± 0.2 % and 0.4 ± 0.0 %, $P = 0.672$). For the degree of conversion, it was statistically non-significant among different materials ($P = 0.087$) (Table 1). However, KeySplint Soft material

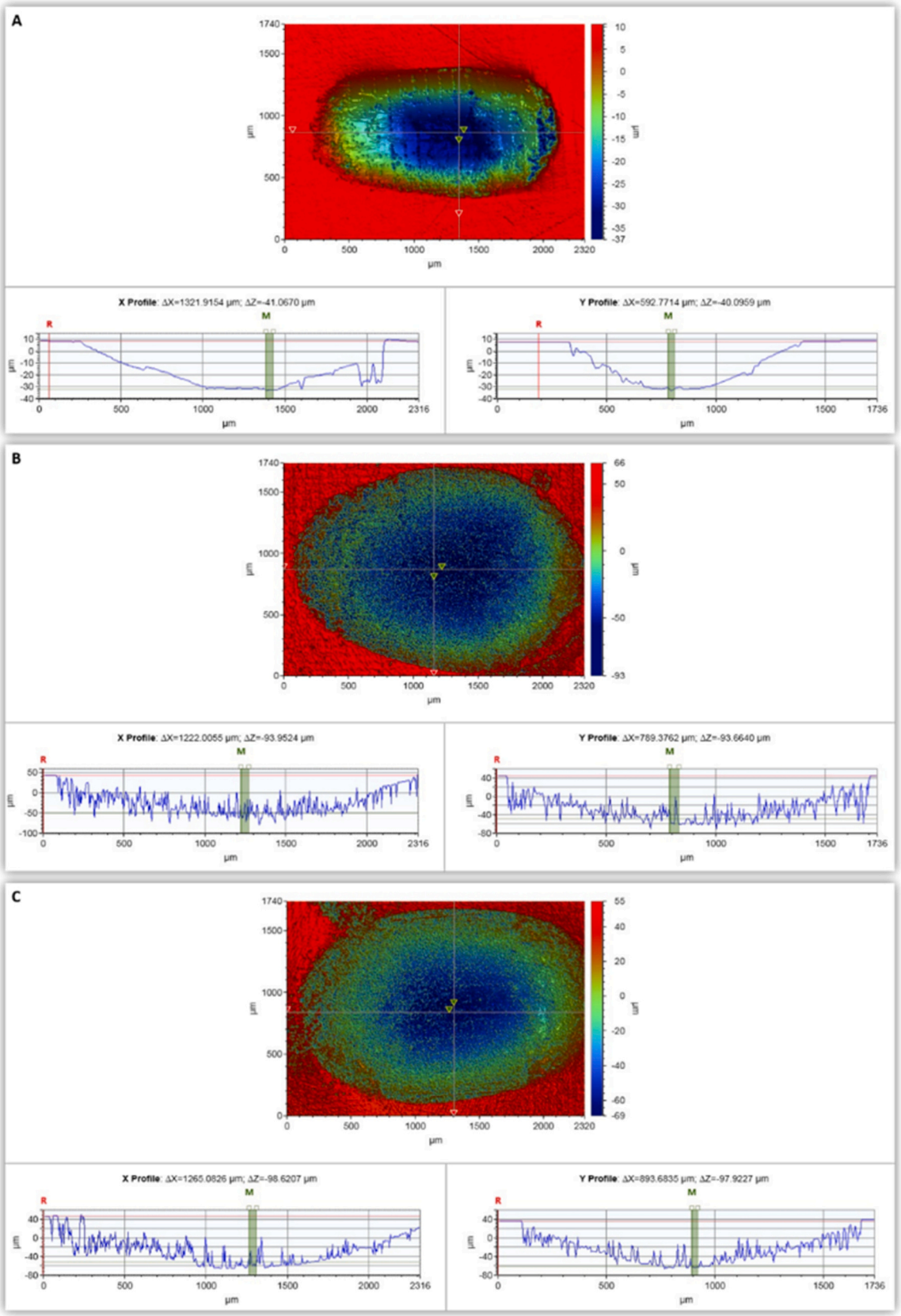

Fig. 4. Wear facets of evaluated 3D-printed flexible splint materials obtained from 3D optical microscope. A, KeySplint Soft; B, IMPRIMO LC Splint flex; C, V-Print splint comfort.

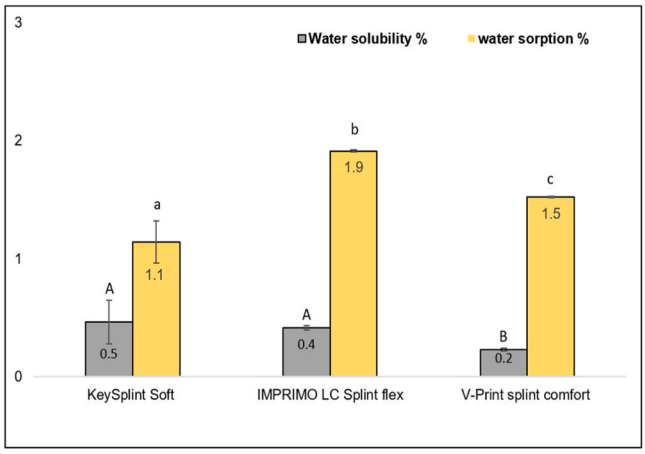

Fig. 5. Mean values of water sorption % and water solubility % of evaluated 3D-printed flexible splint materials. Same letters indicate statistically similar materials ($P > 0.05$). Error bars represent standard deviations.

displayed the highest degree of conversion with 81.8 ± 5.1 %.

4. Discussion

The study's null hypothesis was partially rejected since the characteristics of the tested splint materials differed significantly. However, the dry elastic modulus and the degree of double bond conversion were statistically non-significant among the evaluated materials. All specimens were printed in the same direction, layer thickness, and post-cured using the same device in order to exclude the potential influence of these variables on the mechanical performance of the investigated additively manufactured splint materials [18,31–33].

Flexible 3D printing resins are UV-curable elastomers characterized by low modulus of elasticity and hardness but enhanced flexibility, elongation at break, and elastic rebound [25]. Elastomers' elasticity or stretchability can be explained by the fact that an elastomer is a three-dimensional network of polymer chains cross-linked by strong, covalent chemical bonds. Each chain is made up of a large number of covalently bonded monomers. Between the chains, molecules interact through weak physical bonds, such as hydrogen bonds and van der Waals interaction. Both chemical and physical bonds control the behavior of the elastomer. The covalent bonds between the chain monomers allow them to rotate relative to each other. This rotation enables the chain to take many configurations in response to an imposed load and recover quickly up on load removal. Therefore, an elastomer is considered as an entropic spring [34]. Elongation at break is an indicator of a polymer's ductility since it measures how much bending and shaping a material can withstand before breaking, which is crucial for materials that absorb energy through plastic deformation [35]. According to the manufacturers' technical data, KeySplint Soft had > 110 % elongation at break [36] (ASTM D638 standards [37]), while IMPRIMO LC Splint Flex had > 80 % [38] (DIN 53504 standards [39]), but no value was reported for the V-Print splint comfort.

The investigated splint materials displayed considerable variations in flexural strength, modulus, fracture toughness, and vertical wear, which might be due to the differences in their elemental structures. Usually, the mechanical behavior of photocurable resins is influenced by their chemical composition [3,40–42]. For instance, the first two materials are methacrylate-based, while the last one is acrylate-based, as seen from Table 1. However, it is not clearly explained what kind of methacrylate monomers or oligomers have been used. Unfortunately, the actual chemical makeup of each substance was not explicitly specified in the manufacturers' material safety data sheets (MSDS) for commercial reasons.

One important factor that should be considered in the selection of dental materials in clinical practice is their wear resistance. Interestingly, the wear behavior of the tested materials showed a good connection with the fracture toughness and flexural strength values, which is in good agreement with some literature findings [43,44]. Furthermore, a number of researchers have proposed that fracture toughness and flexural strength could all be indicators of clinical wear [45].

Water storage caused a deterioration of the flexural strength, elastic modulus, and fracture toughness of the investigated materials. However, it was more dramatic for the IMPRIMO LC Splint flex and V-print splint comfort. Those findings were consistent with water sorption, with the IMPRIMO LC Splint flex material exhibiting the highest percentage of water sorption. The uptake of water by resin materials results in a reduction in their mechanical properties [30,46]. Water can interact with resin molecules according to their polarity. The absorbed water acts as a plasticizer, making the material softer. The water-polymer chain interaction can pull the polymer chains away from each other while causing chemical degradation and elution of the residual monomers [30,47]. The microscopic voids between the printed layers may explain why additively manufactured photopolymers absorb more water when compared to the standard autopolymerizing acrylic resin [33]. In addition, the 3D printable flexible splint materials are described as thermo-flexible or with thermo-active memory, meaning that they encounter changes in their room-temperature modulus once exposed to the body temperature or warm water, resulting in a bit of softening and more flexibility for the purpose of improving the patient's compliance. Thus, modulus variations after water storage may also be attributed to the water temperature.

Photocurable resins used in 3D printing are usually comprised of liquid monomers or oligomers and photo-initiators. During the printing process, the photo-initiator is activated by UV light and monomers are converted into polymers, forming polymer chains [48]. However, due to the fast mechanism of layer-by-layer build-up, the intensity of curing through each added layer is insufficient, which eventually minimizes the efficiency of extended chain crosslinking. Therefore, a post-curing cycle is necessarily included to continue the polymerization process, potentially improving the degree of polymerization [49]. FTIR analysis revealed that KeySplint Soft had the highest degree of conversion. Different photo-initiators may influence the degree of resin conversion [50]. Since the manufacturer specifies two alternative wavelengths for KeySplint Soft polymerization, it may be presumed that two photo-initiators are included within its composition to provide an optimized conversion.

Even though none of the tested 3D printed flexible splint materials fractured, their elastic modulus values after water saturation did not surpass 0.5 GPa. It is doubtful if these materials will be able to provide an equal distribution of high occlusal stress on the teeth when used for individuals with parafunctional habits. The clinical implications of the flexibility of digitally created occlusal device materials are not known yet. Therefore, clinical investigations of these new materials are recommended to understand their influence on the stomatognathic system. Furthermore, the significant variation in surface wear behavior among the investigated different materials should be considered when selecting these materials for bruxism patients.

5. Conclusions

1. The mechanical properties of flexible 3D-printed splint materials on the market varied according to their chemical composition.
2. Under dry conditions, the flexural strength of the evaluated flexible 3D-printed splints did not surpass 30 MPa. The elastic modulus was 0.8 GPa. Fracture toughness ranged between 1.1 and 2.3 MPa $m^{1/2}$.
3. Water storage tended to have a significant detrimental effect on the mechanical properties of the evaluated flexible 3D-printed splints.
4. None of the tested splint materials fractured during the flexural strength testing.

5. The degree of double bond conversion for the evaluated flexible 3D-printed splint materials was between 69.4 % and 81.8 %.
6. Among the flexible 3D-printed splint materials tested, KeySplint Soft had the best flexural strength, modulus, fracture toughness, wear resistance, and degree of conversion. Besides, it showed the lowest water sorption.

Authors contributions

The manuscript was written through contributions of all authors. All authors have given approval to the final version of the manuscript.

Acknowledgments

This work was carried out with the financial support provided by the BioCity Turku Biomaterials and Medical Device Research Program.

References

[1] Dylina TJ. A common-sense approach to splint therapy. J Prosthet Dent 2001;86:539–45.
[2] Fricton J, Look JO, Wright E, Alencar Jr FGP, Chen H, Lang M, et al. Systematic review and meta-analysis of randomized controlled trials evaluating intraoral orthopedic appliances for temporomandibular disorders. J Oral Facial Pain Headache 2010;24:237–54.
[3] Wulff J, Schmid A, Huber C, Rosentritt M. Dynamic fatigue of 3D-printed splint materials. J Mech Behav Biomed Mater 2021;124:104885.
[4] Akbulut N, Altan A, Akbulut S, Atakan C. Evaluation of the 3 mm thickness splint therapy on temporomandibular joint disorders (TMDs). Pain Res Manag 2018;2018:3756587.
[5] Riley P, Glenny AM, Worthington HV, Jacobsen E, Robertson C, Durham J, et al. Oral splints for temporomandibular disorder or bruxism: a systematic review. Br Dent J 2020;228:191–7.
[6] Patzelt SBM, Krügel M, Wesemann C, Pieralli S, Nold J, Spies BC, et al. In vitro time efficiency, fit, and wear of conventionally- versus digitally-fabricated occlusal splints. Mater (Basel) 2022;15:1085.
[7] Sriharsha P, Gujjari AK, Dhakshaini MR, Prashant A. Comparative evaluation of salivary cortisol Levels in bruxism patients before and after using soft occlusal splint: an in vivo study. Conte Clin Dent 2018;9:182–7.
[8] Seifeldin SA, Elhayes KA. Soft versus hard occlusal splint therapy in the management of temporomandibular disorders (TMDs). Saudi Dent J 2015;27:208–14.
[9] Coto NP, Brito e Dias R, Costa RA, Antoniazzi TF, de Carvalho EPC. Mechanical behavior of ethylene vinyl acetate copolymer (EVA) used for fabrication of mouthguards and interocclusal splints. Braz Dent J 2007;18:324–8.
[10] Silva CAGD, Grossi ML, Araldi JC, Corso LL. Can hard and/or soft occlusal splints reduce the bite force transmitted to the teeth and temporomandibular joint discs? A finite element method analysis. Cranio J Craniomandib Pr 2020:1–8.
[11] Mertz L. Dream it, design it, print it in 3-D: what can 3-D printing do for you? IEEE Pulse 2013;4:15–21.
[12] Lim SH, Kathuria H, Tan JJY, Kang L. 3D printed drug delivery and testing systems — a passing fad or the future? Adv Drug Deliv Rev 2018;132:139–68.
[13] Habibovic P, Gbureck U, Doillon CJ, Bassett DC, van Blitterswijk CA, Barralet JE. Osteoconduction and osteoinduction of low-temperature 3D printed bioceramic implants. Biomaterials 2008;29:944–53.
[14] Hockaday LA, Kang KH, Colangelo NW, Cheung PYC, Duan B, Malone E, et al. Rapid 3D printing of anatomically accurate and mechanically heterogeneous aortic valve hydrogel scaffolds. Biofabrication 2012;4:035005.
[15] Płatek P, Rajkowski K, Cieplak K, Sarzyński M, Małachowski J, Woźniak R, et al. Deformation process of 3D printed structures made from flexible material with different values of relative density. Polymers 2020;12:2120.
[16] Craveiro F, Duarte JP, Bartolo H, Bartolo PJ. Additive manufacturing as an enabling technology for digital construction: a perspective on construction 4.0. Autom Constr 2019;103:251–67.
[17] du Plessis A, Broeckhoven C, Yadroitsava I, Yadroitsev I, Hands CH, Kunju R, et al. Beautiful and functional: a review of biomimetic design in additive manufacturing. Addit Manuf 2019;27:408–27.
[18] Perea-Lowery L, Gibreel M, Vallittu PK, Lassila L. Evaluation of the mechanical properties and degree of conversion of 3D printed splint material. J Mech Behav Biomed Mater 2021;115:104254.
[19] Berli C, Thieringer FM, Sharma N, Müller JA, Dedem P, Fischer J, et al. Comparing the mechanical properties of pressed, milled, and 3D-printed resins for occlusal devices. J Prosthet Dent 2020;124:780–6.
[20] Wickramasinghe S, Do T, Tran P. FDM-based 3D printing of polymer and associated composite: a review on mechanical properties, defects and treatments. Polymers 2020;12:1529.
[21] Tandon P, Pandey PM, Kumar N, Jain PK. 3D printing of flexible parts using EVA material. Mater Phys Mech 2018;62:124–32.
[22] Woo SG, Lee IH, Lee KC. Hybrid fabrication process of additive manufacturing and direct writing for a 4×4 mm matrix flexible tactile sensor. J Mech Sci Technol 2015;29:3905–9.
[23] Peele BN, Wallin TJ, Zhao H, Shepherd RF. 3D printing antagonistic systems of artificial muscle using projection stereolithography. Bioinspir Biomim 2015;10:055003.
[24] Strohmeier L, Frommwald H, Schlögl S. Digital light processing 3D printing of modified liquid isoprene rubber using thiol-click chemistry. RSC Adv 2020;10:23607–14.
[25] Patel DK, Sakhaei AH, Layani M, Zhang B, Ge Q, Magdassi S. Highly stretchable and UV curable elastomers for digital light processing based 3D printing. Adv Mater 2017;29:1606000.
[26] ISO 20795-1. Dentistry - Base polymers. Part 1: Denture Base Polymers. Geneva, Switzerland: International Organization for Standardization,; 2013.
[27] Perea-Lowery L, Gibreel M, Vallittu PK, Lassila LV. 3D-printed vs. heat-polymerizing and autopolymerizing denture base acrylic resins. Mater (Basel) 2021;14:5781.
[28] Jiangkongkho P, Arksornnukit M, Takahashi H. The synthesis, modification, and application of nanosilica in polymethyl methacrylate denture base. Dent Mater J 2018;37:582–91.
[29] Figueroa RMS, Conterno B, Arrais CAG, Sugio CYC, Urban VM, Neppelenbroek KH. Porosity, water sorption and solubility of denture base acrylic resins polymerized conventionally or in microwave. J Appl Oral Sci Rev FOB 2018;26:e20170383.
[30] Aati S, Akram Z, Shrestha B, Patel J, Shih B, Shearston K, et al. Effect of post-curing light exposure time on the physico–mechanical properties and cytotoxicity of 3D-printed denture base material. Dent Mater 2022;38:57–67.
[31] Reymus M, Lümkemann N, Stawarczyk B. 3D-printed material for temporary restorations: Impact of print layer thickness and post-curing method on degree of conversion. Int J Comput Dent 2019;22:231–7.
[32] Alharbi N, Osman R, Wismeijer D. Effects of build direction on the mechanical properties of 3D-printed complete coverage interim dental restorations. J Prosthet Dent 2016;115:760–7.
[33] Väyrynen VOE, Tanner J, Vallittu PK. The anisotropicity of the flexural properties of an occlusal device material processed by stereolithography. J Prosthet Dent 2016;116:811–7.
[34] Flory PJ. Molecular theory of rubber elasticity. Polym J 1985;17:1–12.
[35] Sakaguchi R, Ferracane J, Powers J. Craig's Restorative Dental Materials. 14th ed..,. St. Louis, Missouri: Elsevier,; 2018. p. 29–68.
[36] Technical Data Sheet. KeySplint Soft. Keystone Industries 2021. ⟨https://keyprint.keystoneindustries.com/wp-content/uploads/2021/09/KeySplint-Soft_Tinted_TDS_R4.pdf⟩. [accessed 28 September 2022].
[37] ASTM D638-14. Standard test method for tensile properties of plastics. West Conshohocken, PA, USA: ASTM International,; 2014.
[38] Technical properties. IMPRIMO System. Scheu Group 2021. ⟨http://products.scheu-dental.com/documents/5000/1-DOC/0/0/0/0/3/IMPRIMO-System_BRO_PM0203_GB_Original_3500.pdf⟩ [accessed 6 October 2022].
[39] DIN 53504. Testing of rubber - Determination of tensile strength at break, tensile stress at yield, elongation at break and stress values in a tensile test; Berlin, Germany 2017.
[40] Lutz AM, Hampe R, Roos M, Lümkemann N, Eichberger M, Stawarczyk B. Fracture resistance and 2-body wear of 3-dimensional–printed occlusal devices. J Prosthet Dent 2019;121:166–72.
[41] Weigel N, Männel MJ, Thiele J. Flexible materials for high-resolution 3D printing of microfluidic devices with integrated droplet size regulation. ACS Appl Mater Interfaces 2021;13:31086–101.
[42] Sarosi C, Moldovan M, Soanca A, Roman A, Gherman T, Trifoi A, et al. Effects of monomer composition of urethane methacrylate based resins on the C=C degree of conversion, residual monomer content and mechanical properties. Polymers 2021;13:4415.
[43] Ferracane JL, Condon JR. In vitro evaluation of the marginal degradation of dental composites under simulated occlusal loading. Dent Mater 1999;15:262–7.
[44] He J, Garoushi S, Säilynoja E, Vallittu PK, Lassila L. The effect of adding a new monomer "Phene" on the polymerization shrinkage reduction of a dental resin composite. Dent Mater 2019;35:627–35.
[45] Heintze SD, Ilie N, Hickel R, Reis A, Loguercio A, Rousson V. Laboratory mechanical parameters of composite resins and their relation to fractures and wear in clinical trials-a systematic review. Dent Mater 2017;33:e101–14.
[46] Gad MM, Rahoma A, Abualsaud R, Al-Thobity AM, Akhtar S, Siddiqui IA, et al. Influence of artificial aging and ZrO2 nanoparticle-reinforced repair resin on the denture repair strength. J Clin Exp Dent 2020;12:e354–62.
[47] Barsby MJ. A denture base resin with low water absorption. J Dent 1992;20:240–4.
[48] Andreescu CF, Ghergic DL, Botoaca O, Hancu V, Banateanu AM, Patroi DN. Evaluation of different materials used for fabrication of complete digital denture. Mater Plast 2018;55:124–8.
[49] Kim D, Shim JS, Lee D, Shin SH, Nam NE, Park KH, et al. Effects of post-curing time on the mechanical and color properties of three-dimensional printed crown and bridge materials. Polymers 2020;12:2762.
[50] Kowalska A, Sokolowski J, Bociong K. The photoinitiators used in resin based dental composite—a review and future perspectives. Polymers 2021;13:470.